Journal of Nuclear Materials 406 (2010) 238–243

Contents lists available at ScienceDirect

Journal of Nuclear Materials

journal homepage: www.elsevier.com/locate/jnucmat

$Gd_2Zr_2O_7$ pyrochlore: Potential host matrix for some constituents of thoria based reactor's waste

B.P. Mandal [a], M. Pandey [b], A.K. Tyagi [a,*]

[a] Chemistry Division, Bhabha Atomic Research Centre, Mumbai 400 085, India
[b] High Pressure and Synchrotron Radiation Physics Division, Bhabha Atomic Research Centre, Mumbai 400 085, India

ARTICLE INFO

Article history:
Received 25 September 2009
Accepted 13 August 2010

ABSTRACT

The present work explores the potential of $Gd_2Zr_2O_7$ for incorporation of ThO_2 and Al_2O_3 which are components of Advanced Heavy Water Reactors (AHWR) waste. XRD studies reveal that the compositions corresponding to y from 0.0 to 0.4 in $Gd_{2-y}Th_yZr_{2-y}Al_yO_7$ are single phasic in nature and beyond $y > 0.4$ the biphasic region starts. The solubility of thoria in $Gd_2Zr_2O_7$ pyrochlore could be enhanced by more than five times by simultaneous incorporation of alumina. The lattice parameter increases with increase in Th and Al content in the series. The r_A/r_B ratio increases with increase in Th and Al content in $Gd_2Zr_2O_7$ and in turn the degree order increases as has been seen by gradual increase in the intensity of superstructure peaks. Single phasic samples were investigated by Raman spectroscopy also. Thermal expansion behavior of single phasic samples was investigated by HT-XRD. In order to confirm the nature of the phases backscattered images have been recorded on all the samples.

1. Introduction

The problem of safe disposal of the nuclear waste especially thorium, aluminium and fluorine, which will be additional components of Advanced Heavy Water Reactors (AHWR) waste, is a challenging task. There is a need to develop modern and safer technologies to incorporate all these nuclear wastes [1]. Several groups all over the world are involved in search for a suitable matrix for the safe disposal of the nuclear wastes [2,3]. A number of materials like glasses, cements, ceramics, etc. are being considered for this purpose. The limitation with borosilicate glass is that it has a tendency to get devitrified in presence of water and steam at high pressure and temperature [2] which may be encountered by glass container after burial in geological repositories. Moreover, water ingression into the geological repositories can cause formation of water soluble salts which may increase the leachability of few species [3]. In addition to that, fixation of actinides and other radwastes in ceramic matrix has several positive aspects like, higher thermodynamic stability, negligible leachability, higher chemical and radiation stability [4]. The host matrix should qualify few stringent thermo physical criteria like it should have low thermal expansion coefficient and high thermal conductivity [5–8].

Pyrochlores are contemplated to be important host matrices for nuclear waste incorporation [9–11]. Pyrochlores have the general formula $A_2B_2O_7$ (S.G. = $Fd\bar{3}m$) where A is the larger cation and B is the smaller one [12]. Interestingly, several workers have described the pyrochlore structure from different angles. Jona et al. [13] and Nyman et al. [14] reported the pyrochlore structure as a network consisting of corner linked of BO_6 octahedra with A atoms at the interstices. Aleshin and Roy [15] and Longo et al. [16] described the pyrochlore structure on the basis of an anion deficient fluorite unit cell. It may be noted that pyrochlore based materials have potential to be used in front end as inert matrix fuel also because its crystal structure permits a wide range of solubility of rare earth elements [10,11], some of them are surrogate materials of minor actinides.

Thoria is going to play an important role as a nuclear fuel in Advanced Heavy Water Reactors (AHWR) in India [17]. In these types of reactors, thorium and aluminium will be generated as additional nuclear wastes and the need of hour is to fix these radwastes, preferably, in a common matrix [18]. It has been found that zirconate pyrochlores, particularly $Gd_2Zr_2O_7$ owing to lower r_A/r_B radius ratio, are extremely stable under high and low energy radiation environments [19,20]. Therefore, we have chosen $Gd_2Zr_2O_7$ as a suitable host material for fixation of waste products. In order to simulate the solubility of minor actinides (MA) in pyrochlore matrix, it has been demonstrated that Ce^{4+} which is surrogate of Pu^{4+}, and Nd^{3+} which is surrogate of Am^{3+}, can be incorporated in $Gd_2Zr_2O_7$ matrix [4,12,21,22]. Additionally, it has also been shown that Sr^{2+}, another waste product can be incorporated in the same matrix [4]. Recently, we have reported that ThO_2 can be incorporated in $Gd_2Zr_2O_7$ though the extent of solubility was limited (till $y = 0.075$ in $Gd_{2-y}Th_yZr_2O_{7+y/2}$) [23]. In continuation, we have attempted to improve the solubility of Th by co-doping

* Corresponding author. Tel.: +91 22 2559 5330; fax: +91 22 2550 5151.
E-mail address: aktyagi@barc.gov.in (A.K. Tyagi).

0022-3115/$ - see front matter © 2010 Elsevier B.V. All rights reserved.
doi:10.1016/j.jnucmat.2010.08.042

of Al at Zr site of $Gd_2Zr_2O_7$ lattice. A simultaneous incorporation of Th and Al in $Gd_2Zr_2O_7$ will ensure charge compensation also. In this manuscript, we report on preparation of Zr and Al substituted $Gd_2Zr_2O_7$ and structural investigation of the products by X-ray diffraction and Raman spectroscopic techniques.

2. Experimental details

AR grade powders of Gd_2O_3, zirconium oxy-nitrate, thorium nitrate, aluminium nitrate and glycine were used as the starting reagents. Gd_2O_3 were pre-heated at 700 °C for overnight to remove moisture and other volatile impurities, if any. Subsequently, it was dissolved in minimum amount of dil. HNO_3. The net oxidizing valency of gadolinium nitrate, thorium nitrate, zirconium oxy-nitrate and aluminium nitrate and reducing valencies of fuel were calculated using the valencies of individual elements [24]. In order to obtain different compositions of $Gd_{2-y}Th_yZr_{2-y}Al_yO_7$ ($0.0 \leqslant y \leqslant 2.0$), required amounts of metal nitrates were mixed in proper ratio. Glycine has been used as a fuel in this reaction. These solutions, after thermal dehydration (at ≈80 °C) on a hot plate, resulted a highly viscous liquid. As soon as the viscous liquid was formed, the temperature of the hot plate was increased to ≈200 °C. At this stage the viscous liquid swelled and auto-ignited, with the rapid evolution of large volume of gases to produce voluminous powders. In order to remove the decomposition products and excess carbon, the powders obtained after auto-ignition were calcined at 600 °C for 45 min. In order to investigate the phase formation process the samples have been annealed at different temperatures. The final sintering has been done for all the samples at 1430 °C for 12 h.

XRD has been recorded on the calcined powders using monochromatized Cu Kα radiation on a Philips X-ray diffractometer, Model PW 1927. The microstructure of the sintered pellets was investigated using AIS 210 scanning electron microscope (Mirero Inc., Korea). No coating was given to the samples. The backscattered images have been taken in order to investigate the nature of the phases. The Raman spectra were recorded using a 532 nm line from a solid state Nd:YAG laser and the scattered light was analyzed using a single stage 0.9 m spectrograph (with notch filter) and back thinned CCD detector for >100 cm^{-1}.

3. Results and discussion

Earlier limited solubility of thoria in $Gd_2Zr_2O_7$ lattice has been reported [23]. Incorporation of Th^{4+} at Gd^{3+} site of $Gd_2Zr_2O_7$ results an introduction of excess anions in $Gd_{2-y}Th_yZr_2O_{7+y/2}$ lattice. The presence of excess anions in the lattice leads to early phase separation in the series and thus restricts the solubility of Th^{4+} up to $y = 0.075$ only. In the present work, we have made attempts to increase the solubility of Th^{4+} in $Gd_2Zr_2O_7$ by substituting Al^{3+} at Zr^{4+} site of $Gd_2Zr_2O_7$. The substitution of Al^{3+} at Zr^{4+} site can compensate the extra oxygen resulted due to incorporation of Th^{4+} at Gd^{3+} site, which is expected to increase the solubility of Th^{4+} in $Gd_2Zr_2O_7$.

XRD patterns of all the products in $Gd_{2-y}Th_yZr_{2-y}Al_yO_7$ ($0.0 \leqslant y \leqslant 2.0$) series were recorded and analyzed. A few representative XRD patterns are shown in Fig. 1. The parent $Gd_2Zr_2O_7$ crystallizes as pyrochlore which is evident by the presence of super-lattice peaks at $2\theta \approx 14°(1\,1\,1)$, $27°(3\,1\,1)$, $37°(3\,3\,1)$, $45°(5\,1\,1)$ (using Cu Kα as radiation source). It is observed from Fig. 1 that the compositions corresponding to $y = 0.0$–0.4 adopt a pyrochlore structure. A systematic shift of the diffraction peaks towards lower angle on Th and Al incorporation (Fig. 1) clearly indicates that the cell parameters of the doped pyrochlores increase as the content of Th and Al increase. The cell parameters of all the compositions were

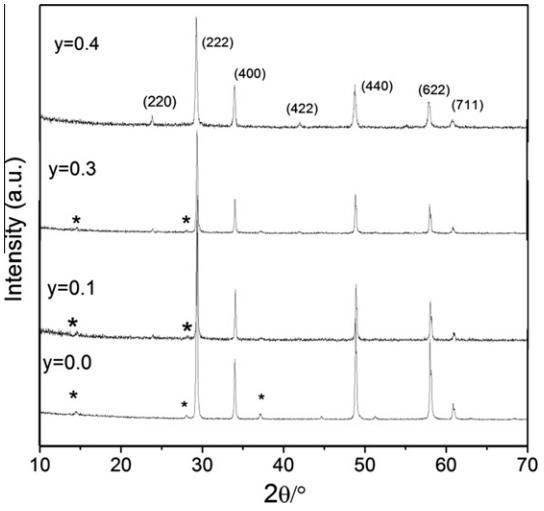

Fig. 1. XRD patterns of single phasic compositions in the $Gd_{2-y}Th_yZr_{2-y}Al_yO_7$ systems in the range $0.0 \leqslant y \leqslant 0.4$ (asterisks indicate the superstructure peaks).

calculated using POWDERX program which show an increasing trend as a function of Th and Al content up to $y = 0.4$ (Fig. 2). In our earlier study [23], it has been observed that the compositions were single phasic till $y = 0.075$ in $Gd_{2-y}Th_yZr_2O_{7+y/2}$. It is remarkable to note that the solubility of Th^{4+} increased by more than five times as the compositions till $y = 0.4$, are found to be single phasic in nature. The considerably increased solubility of Th^{4+} in $Gd_2Zr_2O_7$ is attributed to simultaneous incorporation of Al^{3+} at Zr^{4+} site which takes care of charge compensation thus preventing the introduction of excess anions in the pyrochlore lattice.

Fig. 3 demonstrates the XRD patterns of $Gd_2Zr_2O_7$ at different temperatures. The XRD pattern of the calcined powder is broad enough and it is difficult to conclude about the degree of ordering of the system. With increase in temperature the peaks become narrower which is evident from Fig. 3. The XRD pattern recorded for the sample heated at 1430 °C shows superstructure peaks. The superstructure peaks are also visible in the XRD pattern of the sample sintered at 1430 °C.

An interesting result has been observed in the trend of cell parameters of the samples. The ionic radii of Gd^{3+} and Th^{4+}, in 8-fold coordination, are 1.05 Å and 1.05 Å and the ionic radii of Zr^{4+} and Al^{3+} are 0.72 Å and 0.54 Å in six fold coordinate [25]. Therefore,

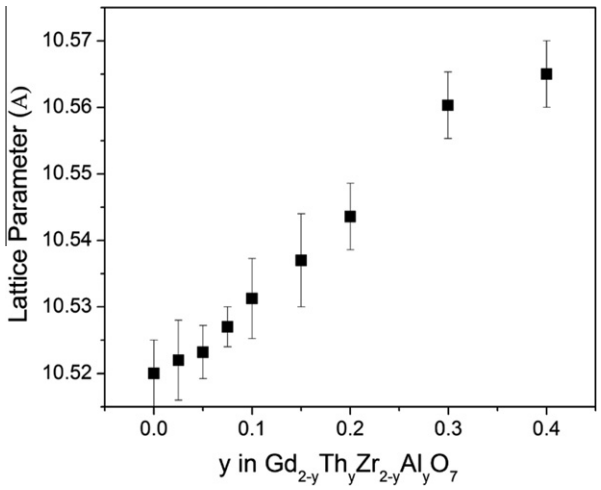

Fig. 2. Variation of room temperature lattice parameter with change in compositions in $Gd_{2-y}Th_yZr_{2-y}Al_yO_7$ series.

a simultaneous incorporation of Th^{4+} and Al^{3+} at Gd^{3+} and Zr^{4+} site, respectively, should result a decrease in cell parameters. However, the cell parameter increases in $Gd_{2-y}Th_yZr_{2-y}Al_yO_7$ series on increasing y. The probable reason may be that part of Al^{3+} is residing at some of interstitial sites of host pyrochlore. In our previous study also we found that with the incorporation of Th^{4+} at Gd^{3+} site in $Gd_2Zr_2O_7$, there was an increase in lattice parameter, which was due to extra oxygen incorporation in the lattice [23]. Qu et al. [26] have shown that when $Sm_2Zr_2O_7$ was substituted with MgO (till $y = 0.075$ in $Sm_{2-y}Mg_yZr_2O_{7-y/2}$), it resulted in an increase in the lattice parameter of the solid solution, though the ionic radii of Mg^{2+} is smaller than that of Sm^{3+}. They attributed this increase in cell parameter to the repulsion amongst the dopants incorporated at the interstitial sites. Perhaps in the present investigation also, during the course of substitution some interstitial sites are occupied by smaller Al^{3+} ions resulting in an increase in the cell parameter due to an electrostatic repulsion.

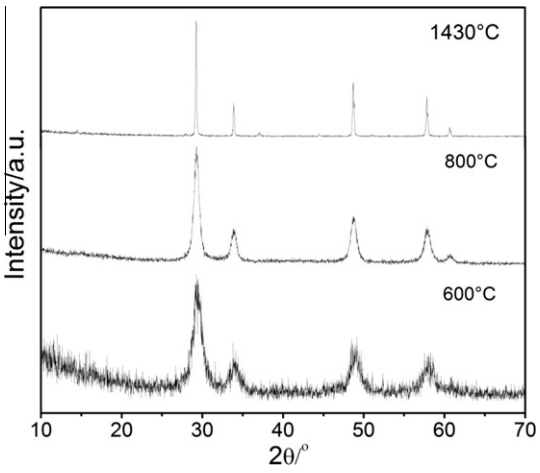

Fig. 3. XRD patterns of $Gd_2Zr_2O_7$ at 600 °C, 800 °C and 1430 °C.

Table 1
Intensity of (2 2 0), (4 2 2) and (6 2 2) planes with respect to (2 2 2) plane.

	0.0	0.025	0.05	0.075	0.1	0.15	0.2	0.3	0.4
I_{220}	~0%	~0%	0.61	0.98	1.78	2.20	3.58	5.91	6.84
I_{422}	~0%	~0%	~0%	0.47	0.85	0.95	1.09	2.14	5.01
I_{622}	~0%	~0%	~0%	0.51	0.57	0.73	0.85	1.1	1.2

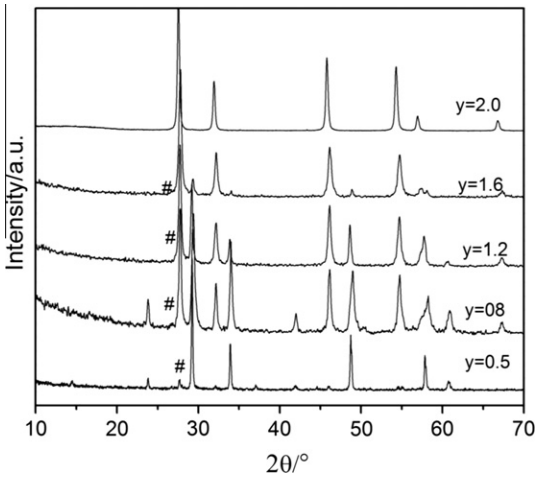

Fig. 4. XRD patterns of the compositions in the $Gd_{2-y}Th_yZr_{2-y}Al_yO_7$ systems in the range $0.5 \leqslant y \leqslant 2.0$.

The cations and anions in pyrochlore structure become more and more ordered with increase in r_A/r_B ratio. Dickson et al. [27] reported that the planes like (2 2 0), (4 2 2), etc. consists of anions and the planes like (6 2 2). consists of metal ions only. The interesting observation is that the intensity of all the superstructure peaks increases with increase in Th^{4+} and Al^{3+} content. The increase in intensity of the peaks corresponding to planes consisting of only oxygens like (2 2 0), (4 2 2), etc. with increase in r_A/r_B ratio is a rare observation in pyrochlores. The plausible reason could be that with increase in r_A/r_B ratio the degree of order increased to such an extent that the intensity of oxygen ordered peaks becomes stronger. The intensities of these peaks with respect to 100% peak (2 2 2) have been tabulated in the Table 1. It may be noted that the superstructure peaks in most of the pyrochlores are too feeble to observe by lab source XRD. Thus the present series of pyrochlores is a rare example wherein even the superstructure peaks due to anionic ordering are also observed.

From the composition $y = 0.5$ onward, biphasic regime comprising of pyrochlore phase and F-type phase starts appearing (Fig. 4). This F-type phase is a solid solution of ThO_2 and Al_2O_3. The cell parameter of this F-type phase is found to be 5.578(6) Å through out the biphasic region ($y = 0.5$–1.6). The peak intensity of secondary phase increases with increase in Th^{4+} and Al^{3+} content in the series. It can be seen form Fig. 4 that the composition corresponding to $y = 2.0$ is single phasic in nature. The lattice parameters of the compositions corresponding to $y = 2.0$ is found to be 5.524(3) Å. Since the ionic radius of Al^{3+} is smaller than that of Th^{4+} therefore, the lattice parameter of the composition corresponding to $y = 2.0$ was smaller than pure ThO_2 ($a = 5.597$ Å).

In order to investigate the thermal expansion behavior, XRD data were recorded on few selected samples over the temperature range 25–1000 °C. The lattice parameters at each temperature were refined (Table 2). The samples are tacitly chosen only from the monophasic region. As expected, initially the lattice parameter increases almost linearly with temperature but it shows a deviation from linearity at higher temperatures due to contribution from the nonlinear terms. The linear coefficient of thermal expansion (α) has been estimated (Table 2) for representative samples from the mean variation of their lattice parameters at low

Table 2
Lattice parameters at different temperature and thermal expansion coefficient in $Gd_{2-y}Th_yZr_{2-y}Al_yO_7$ system.

Temperature (K)	y in $Gd_{2-y}Th_yZr_{2-y}Al_yO_7$				
	0	0.075	0.1	0.15	0.2
298	10.520(5)	10.527(3)	10.531(4)	10.537(5)	10.543(4)
473	10.537(4)	10.539(4)	10.539(5)	10.541(3)	10.553(3)
673	10.561(3)	10.561(3)	10.563(5)	10.564(5)	10.576(4)
873	10.586(5)	10.590(5)	10.583(6)	10.592(3)	10.601(4)
1073	10.616(6)	10.616(3)	10.624(2)	10.625(5)	10.626(5)
1273	10.640(8)	10.644(4)	10.649(3)	10.652(4)	10.656(3)
Cooled to RT	10.520(3)	10.525(4)	10.530(3)	10.538(4)	10.543(3)
Thermal expansion coefficient $\times 10^6$ (K^{-1})	11.4	11.34	11.25	11.13	10.91

temperatures according to the equation $\alpha = \{(a - a_0)/a_0\Delta T\}$ where 'a_0' and 'a' denote lattice parameter at room temperature and at any given temperature (T), and ΔT is the difference between the two temperatures. It is well known that thermal expansion coefficient decreases with increase in covalency in a series of compositions. In the present investigation also, it has been found that with increase in Al content in the compositions, thermal expansion coefficient decreases because the degree of covalency increases with increase in Al–O content in the series [28].

In order to further confirm the phase information of the compositions, backscattered electron imaging has been performed on the samples. Fig. 5a–f shows the backscattered electron images (BEI) of the single phasic and biphasic samples of $Gd_{2-y}Th_yZr_{2-y}Al_yO_7$ series. The surface of the samples was polished. Since the samples were sintered at very high temperature (1430 °C); the porosity decreases significantly. However, highly dense samples could not be prepared even at this temperature also. Backscattered electron images on the samples having compositions till $y = 0.4$ indicate that the compositions are single phasic in nature which corroborate XRD result.In the biphasic region also pores could not be removed completely by repeated heating. Bright and grey phases which correspond to higher Z and lower Z phase in the samples

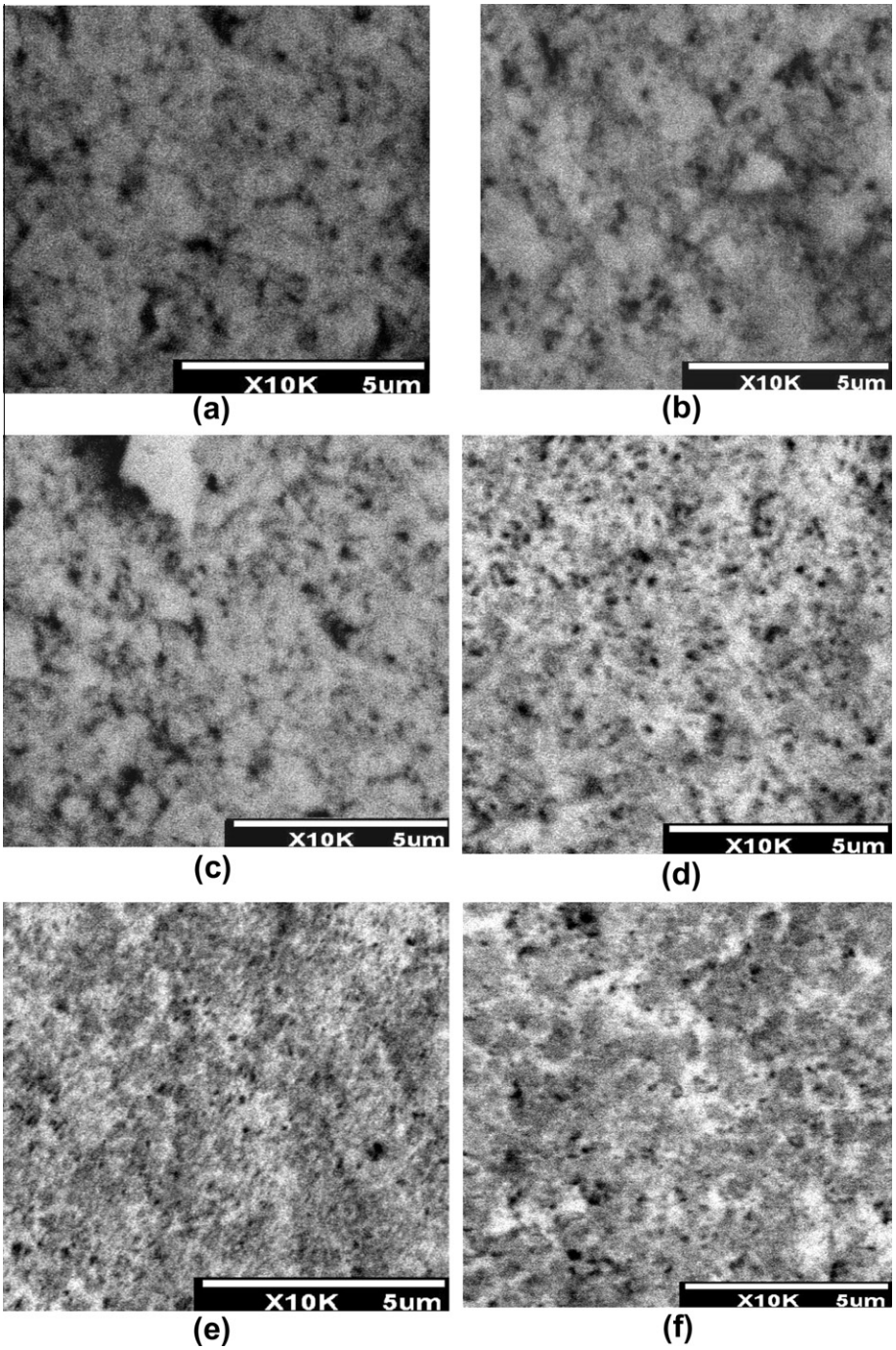

Fig. 5. Backscattered electron images of (a) pure $Gd_2Zr_2O_7$, (b) $Gd_{1.8}Th_{0.2}Zr_{1.8}Al_{0.2}O_7$, (c) $Gd_{1.6}Th_{0.4}Zr_{1.6}Al_{0.4}O_7$, (d) $Gd_{1.5}Th_{0.5}Zr_{1.5}Al_{0.5}O_7$, (e) $Gd_{0.8}Th_{1.2}Zr_{0.8}Al_{1.2}O_7$, (f) $Gd_{0.4}Th_{1.6}Zr_{0.4}Al_{1.6}O_7$.

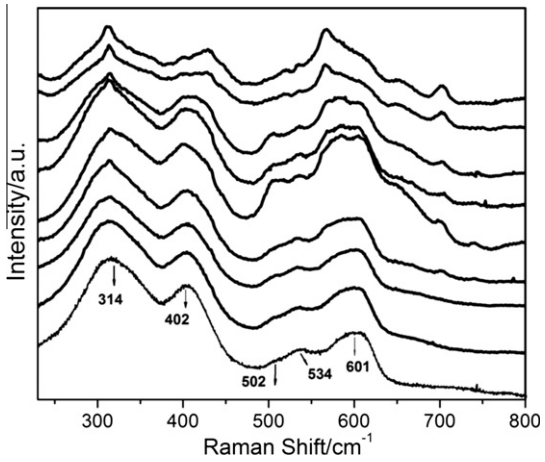

Fig. 6. Raman spectra of the single phasic samples in $Gd_{2-y}Th_yZr_{2-y}Al_yO_7$ series. (a) $y = 0.0$, (b) $y = 0.025$, (c) $y = 0.05$, (d) $y = 0.075$, (e) $y = 0.1$, (f) $y = 0.15$, (g) $y = 0.2$, (h) $y = 0.3$, (i) $y = 0.4$.

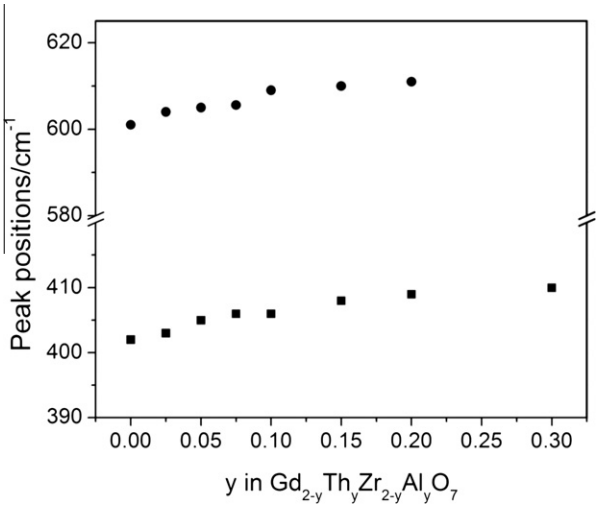

Fig. 7. Change in peak position of the peaks at 400 cm^{-1} and 602 cm^{-1} with change in compositions.

$y = 0.5–1.6$ could be observed. XRD investigation also revealed that these compositions ($y = 0.5–1.6$) are biphasic only.

X-ray diffraction studies are more useful to know about the disorder in the cationic sublattice in comparison with anionic sublattice because of high atomic number of the cation compared to oxygen. On the other hand, Raman spectroscopy is very much sensitive to oxygen polarizability and local coordination. It has been reported in literature that Raman spectroscopic studies can be used explicitly [29] to differentiate among highly ordered and disordered pyrochlore. All the single phasic compositions were further investigated by Raman spectroscopy over the frequency range 200–800 cm^{-1} to identify the degree of order and disorder in the systems. Cubic pyrochlore, $A_2B_2O_7$, belongs to space group ($Fd\bar{3}m$, O_h^7) with $Z = 8$ has six Raman active modes and seven IR active modes which can be represented as [26,29]

$$\Gamma = A_{1g} + E_g + 4T_{2g} + 7T_{1u}$$

Among these modes, the Raman active modes are $A_{1g} + E_g + 4T_{2g}$ [30]. All the six modes of pyrochlores have been found in the Raman spectra which are shown in Fig. 6. The observed peaks are at 314, 402, 502, 534 and 601 cm^{-1} for $Gd_2Zr_2O_7$ compounds. They match reasonably well with the reported spectra [12]. The band assignment in the present study has been done following Vandenbore's Raman spectroscopy work on pyrochlores [30] (Table 3). However, they had observed two separate modes at 523 and 532 cm^{-1}, whereas in present study we observed two bands at 502 and 534 cm^{-1} for $Gd_2Zr_2O_7$ using least square fitting. The band at 314 cm^{-1} has been assigned to E_g mode following our earlier work [30,31]. The peak at 534 cm^{-1} is assigned to A_{1g} mode since its intensity changes significantly with different directions of polarization [30,32,33]. The other bands at 402, 502, 601 cm^{-1} are due to T_{2g} modes of the cubic pyrochlore structure. A broad peak at ~710 cm^{-1} has been observed in the spectra specially $y = 0.075$ onwards. In our earlier work also we found that a hump at 730 cm^{-1} and it had been argued that it may be due to distortion of the octahedra or to the combination bands [30] or it could be due to the forbidden modes as assigned by Ouselati et al. [34]. It is observed that the peaks are very broad in all the samples and with increase in dopant concentration the peaks become broader. The host matrix, i.e. $Gd_2Zr_2O_7$ is highly disordered pyrochlore as it has been reported earlier [12]. This broadening isn't attributed to the smaller particle size because the samples were sintered at 1200 °C for 4 h and the XRD patterns shows very sharp peaks which indicate the size of the particles are in micro regime. As mentioned earlier that pyrochlore is ordered modification of fluorite structure having a vacancy at one oxygen site. Due to presence of vacancy, defects and foreign ions, disruption in the translational symmetry in the lattice takes place and consequently it relaxes the $k \approx 0$ selection rule. Therefore, phonons from all parts of the Brillouin zone are allowed to contribute to the optical spectra, which ultimately give rise to broadened, continuously spread peaks, as observed in the present study.

The intensity of the peak at 314 cm^{-1} (E_g) decreases with increase in concentration of Th^{4+} and Al^{3+} in the solid solution. On the other hand, the intensity of the Raman peak at 400 cm^{-1} (T_{2g}) remains almost unchanged but its position shifts slightly towards higher wavenumber. Another peak at 601 cm^{-1} also shows blue shift with increase in Th and Al content in the series. From Table 3, it can be seen that these two peaks are due to B–O stretching in $A_2B_2O_7$ structure. The reason may be that with increase in Al content in the series the B–O bond becomes stronger and the Raman peak appears at higher frequency (Fig. 7).

Table 3
Raman mode frequencies with symmetry character and vibration types in $A_2B_2O_7$ pyrochlores.

Frequency (cm^{-1})	Symmetry	Vibration type
314	E_g	$B–O_6$ bending
402	T_{2g}	Mostly B–O stretch with mixture of A–O stretch and O–B–O bending vibrations
502	T_{2g}	Mostly O–B–O bend with mixture of B–O and A–O stretch
523	A_{1g}	Mostly O–B–O bend
601	T_{2g}	Mostly B–O stretch
710		Distortion in octahedra or combination of band [Ref. 30]

4. Conclusions

In this investigation, a series of compositions with general composition $Gd_{2-y}Th_yZr_{2-y}Al_yO_7$ ($0 \leqslant y \leqslant 2.0$) were prepared by a gel combustion method and characterized by XRD and Raman spectroscopy. It was found that the samples are single phasic pyrochlores till $y = 0.4$. The lattice parameter increases with increase in Th and Al content in the series up to $y = 0.4$. Back scattered images also indicate that the secondary phases can be seen in the samples

$y = 0.5$ onwards. Hence, it can be concluded that the simultaneous incorporation of Al to Th in $Gd_2Zr_2O_7$ has two distinct advantages. Firstly, the solubility of thoria in $Gd_2Zr_2O_7$ lattice increases more than five fold. Additionally Al, which is a constituent of AHWR waste, can also be immobilized.

Acknowledgement

Authors are thankful to Dr. C.G.S. Pillai and Mr. J. Nuwad, ChD, BARC for their help in SEM recording and fruitful discussion.

References

[1] H. Kleycamp, J. Nucl. Mater. 275 (1999) 1.
[2] G.J. McCarthy, W.B. White, R. Roy, B.E. Scheetz, S. Komarzeni, D.S. Smith, D.M. Roy, Nature 273 (1978) 216.
[3] A.E. Ringwood, S.E. Kesson, N.G. Ware, W. Hibberson, A. Major, Nature 278 (1979) 219.
[4] S.J. Patwe, A.K. Tyagi, Ceram. Inter. 32 (2006) 545.
[5] J.M. Paratte, R. Chawla, Ann. Nucl. Energy 22 (1995) 471.
[6] M. Burghartz, H. Matzke, C. Leger, V. Vambenepe, M. Roma, J. Alloys Compd. 271 (1998) 544.
[7] K. Ferguson, Trans. Am. Nucl. Soc. 75 (1996) 75.
[8] I. Hayakawa, H. Kamizono, J. Nucl. Mater. 202 (1993) 163.
[9] K.E. Sickafus, L. Minervini, R.W. Grimes, J.A. Valdez, M. Ishimaru, F. Li, K.J. McClellan, T. Hartmann, Science 289 (2000) 748.
[10] R.C. Ewing, W.J. Weber, J. Lian, J. Appl. Phys. 95 (2004) 5949.
[11] S. Lutique, D. Staicu, R.J.M. Konings, V.V. Rondinella, J. Somers, T. Wiss, J. Nucl. Mater. 319 (2003) 59.
[12] B.P. Mandal, A. Banerji, V. Sathe, S.K. Deb, A.K. Tyagi, J. Solid State Chem. 180 (2007) 2643.
[13] F. Jona, G. Shirane, R. Pepinsky, Phys. Rev. 98 (1955) 903.
[14] H. Nyman, S. Andersson, B.G. Hyde, M. O'Keeffe, J. Solid State Chem. 26 (1978) 123.
[15] E. Aleshin, R. Roy, J. Am. Ceram. Soc. 45 (1962) 18.
[16] J.M. Longo, P.M. Raccah, J.B. Goodenough, Mater. Res. Bull. 4 (1969) 191.
[17] A. Kakodkar, Shaping the third stage of Indian Nuclear Power Programme, Presented at 12th Annual Conference of Indian Nuclear Society (INSAC- 2001), Indore, India.
[18] B. Bhattacharjee, An Overview of R&D in Fuel Cycle Activities of AHWR, INSAC 2003, Kalpakkam IT 1/26.
[19] J. Lian, X.T. Zu, K.V.G. Kutty, J. Chen, L.M. Wang, R.C. Ewing, Phys. Rev. B 66 (2002) 054108.
[20] S.X. Wang, B.D. Begg, L.M. Wang, R.C. Ewing, W.J. Weber, K.V. Govindan Kutty, J. Mater. Res. 14 (1999) 4470.
[21] Z.-G. Liu, J.-H. Ouyang, Y. Zhou, J. Mater. Sci. 43 (2008) 3596.
[22] B.P. Mandal, A.K. Tyagi, J. Alloys Compd. 437 (2007) 260.
[23] B.P. Mandal, Nandini Garg, S.M. Sharma, A.K. Tyagi, J. Nucl. Mater. 392 (2009) 95.
[24] J.J. Kingsley, K. Suresh, K.C. Patil, J. Mater. Sci. 25 (1990) 1305.
[25] R.D. Shannon, Acta Cryst. A32 (1976) 751.
[26] Z. Qu, C. Wan, W. Pan, Chem. Mater. 19 (2007) 4913.
[27] S.J. Dickson, K.D. Hawkings, T.J. White, J. Solid State Chem. 82 (1989) 146.
[28] A.K. Tyagi, M.D. Mathews, R. Ramachandran, J. Nucl. Mater. 294 (2001) 198.
[29] M. Glerup, O.F. Nielsen, F.W. Poulsen, J. Solid State Chem. 160 (2001) 25.
[30] M.T. Vandenborre, E. Husson, J.P. Chatry, D. Michel, J. Raman Spectrosc. 14 (1983) 63.
[31] B.E. Scheetz, W.B. White, J. Am. Ceram. Soc. 62 (1979) 468.
[32] N.J. Hess, B.D. Begg, S.D. Conradson, D.E. McCready, P.L. Gassman, W.J. Weber, J. Phys. Chem. B 106 (2002) 4663.
[33] F.X. Zhang, B. Manoun, S.K. Saxena, C.S. Zha, Appl. Phys. Lett. 86 (2005) 181906.
[34] M. Oueslati, M. Balkanski, P.K. Moon, H.L. Tuller, Mater.Res. Soc. Sympos. Proc. 135 (1989) 199.